Experimental Research

ANNALS OF MEDICINE & SURGERY

OPEN

Screening of diagnostic biomarkers for ferroptosis-related osteoarthritis and construction of a risk-prognosis model

Yiqun Yan, MSc[a,b], Junyan He, MSc[a,b], Wendan Cheng, PhD[a,b,*]

Background: Osteoarthritis (OA) is the most prevalent and commonly chronic joint disease that frequently develops among the elderly population. It is not just a single tissue that is affected, but rather a pathology involving the entire joint. Among them, synovitis is a key pathological change in OA. Ferroptosis is a newly discovered form of cell death that results from the buildup of lipid peroxidation. However, the role and impact of it in OA are yet to be explored.

Objective: The key to this work is to uncover the mechanisms of ferroptosis-related OA pathogenesis and develop more novel diagnostic biomarkers to facilitate the diagnostic and therapeutic of OA.

Materials and methods: Download ferroptosis-related genes and OA synovial chip datasets separately from the FerrDB and Gene Expression Omnibus databases. Identify ferroptosis differentially expressed genes using R software, obtain the intersection genes through two machine learning algorithms, and obtain diagnostic biomarkers after logistic regression analysis. Verify the diagnostic and therapeutic efficacy of specific genes for OA through the construction of clinical risk prognostic models using ROC curves and nomogram. Simultaneously, correlations between specific genes and OA immune cell infiltration co-expression were constructed. Finally, verify the differential presentation of specific genes in OA and health control synovium.

Results: Obtain 38 ferroptosis differentially expressed genes through screening. Based on machine learning algorithms and logistic regression analysis, select AGPS, BRD4, RBMS1, and EGR1 as diagnostic biomarker genes. The diagnostic and therapeutic efficacy of the four specific genes for OA has been validated by ROC curves and nomogram of clinical risk prognostic models. The analysis of immune cell infiltration and correlation suggests a close association between specific genes and OA immune cell infiltration. Further revealing the diagnostic value of specific genes for OA by the differential presentation analysis of their differential presentation in synovial tissue from OA and health control.

Conclusion: This study identified four diagnostic biomarkers for OA that are associated with iron death. The establishment of a risk-prognostic model is conducive to the premature diagnosis of OA, evaluating functional recovery during rehabilitation, and guidance for subsequent treatment.

Keywords: bioinformatics analysis, biomarker, differentially expressed genes, GEO, osteoarthritis

Introduction

Osteoarthritis (OA) is the most prevalent and commonly chronic joint disease that frequently develops among the elderly population. It is not just a single tissue that is affected, but rather a whole joint disorder that mainly involves progressive destruction of joint cartilage, sustained low-grade inflammation of the synovium, injury and remodeling of subchondral bone, and formation of osteophytes in the joint space[1,2]. There are many factors that can contribute to the pathogenesis of OA, including age, sex, genetics,

HIGHLIGHTS

I will outline our study across several dimensions:

- In this study, we utilized the LASSO and SVM-RFE machine learning algorithms for the first time to screen differentially expressed genes, which greatly improved the representativeness of the screened genes.
- Subsequently, we conducted univariate and multivariate analyses on the intersection genes identified by both algorithms using logistic regression analysis, which further improved the practical clinical value of the screened genes.
- Finally, four specific genes that were positively identified by both univariate and multivariate analyses were selected as diagnostic biomarkers. Furthermore, by constructing ROC curves and column charts for clinical risk prognostic models, the four diagnostic biomarker genes were further determined to have a good diagnostic and therapeutic effect on osteoarthritis.

[a]Department of Orthopedics and [b]Institute of Orthopedics, Research Center for Translational Medicine, The Second Affiliated Hospital of Anhui Medical University, Hefei 230601, Anhui province, People's Republic of China

Sponsorships or competing interests that may be relevant to content are disclosed at the end of this article.

*Corresponding author. Address: Second Affiliated Hospital of Anhui Medical University, 合肥市, 安徽省 People's Republic of China. Tel.: +86 13230651976. E-mail: chenwendan@ahmu.edu.cn (W. Cheng).

Annals of Medicine & Surgery (2024) 86:856–866

Received 29 September 2023; Accepted 24 December 2023

Published online 4 January 2024

http://dx.doi.org/10.1097/MS9.0000000000001696

body weight, and more[3]. However, it is undeniable that OA is a silent disease before typical symptoms and imaging changes appear. During the lengthy subclinical period, joint cartilage may have already undergone irreversible damage and changes[4,5]. Therefore, further screening of ferroptosis-related genes (FRGs) in OA patients may provide potential therapeutic targets. Also facilitates research into the mechanics of OA.

Ferroptosis is an iron-mediated type of cellular demise that occurs due to the assembly of lipid peroxidation resulting from the action of divalent iron on highly expressed unsaturated fatty acids on the cell membrane[6]. This creates its fundamental difference with necrosis, autophagy, and apoptosis[7]. Newly, ferroptosis has evolved into a research hotspot for diseases like cardiovascular disease, kidney injury, and cancer[8–10]. Some have also suggested that ferroptosis plays a crucial role in the onset and progression of OA, but its exact pathogenesis is still unclear[11]. With the advancement of research on ferroptosis and related biological processes (BP), targeting interventions in ferroptosis and its related pathways may become an efficacious strategy for ministering OA[12]. Therefore, further screening of FRGs among OA patients could potentially reveal viable targets for healing intervention.

This work used bioinformatics methods to analyze four Gene Expression Omnibus (GEO) datasets (GSE82107, GSE55235, GSE55457, and GSE12021) and screened for ferroptosis differentially expressed genes (FDEG) in synovial tissues from OA and healthy control (HC) groups. By using two machine learning algorithms and logistic regression analysis, four diagnostic biomarker genes, AGPS, BRD4, RBMS1, and EGR1 were identified. The diagnostic and therapeutic effects of these biomarkers on OA were validated through ROC curve and nomogram clinical risk prognosis models. Simultaneously, correlations between specific genes and OA immune cell infiltration co-expression were constructed. Finally, verify the differential presentation of specific genes between OA and HC synovium will be validated to further reveal their diagnostic value for OA. This work seeks to uncover the pathogenic mechanism of OA connected to ferroptosis and develop additional diagnostic biological markers for reference.

Materials and methods

Data source and acquisition of differentially expressed genes (FDEG)

Retrieve the OA synovial chip dataset from the GEO database.

Download the GSE12021, GSE55457, and GSE55235 datasets from the GPL96 platform, which uses the Affymetrix Human Genome U133A array, as well as the GSE82107 dataset from the GPL570 platform, which uses the Affymetrix Human Genome U133 Plus 2.0 array. This will provide synovial gene transcription profiles and relevant clinical information for 50 OA and 40 points of HC cases. Apply the 'SVA' package and 'limma' package to adjust for batch effects and perform standardized integration of the datasets for further analysis[13,14].

Collected FRGs from the FerrDB database. A total of 728 FRGs were included, including Diver group genes, Suppressor group genes, and Marker group genes.

On this basis, the 'limma' package was used to filter for FDEGs in the synovial membranes of OA and HC, with a standard set at $P < 0.05$ and $|\log FC| > 1$.

Functional enrichment analysis

Functional enrichment analysis of FDEGs was conducted using Gene Ontology (GO) and Kyoto Encyclopedia of Genes and Genomes (KEGG) through the application of the 'clusterProfiler' and 'enrichplot' packages, with a standard set at $P < 0.05$ and $q < 0.05$ as statistically meaningful differences[15]. The GO terms included BP, molecular functions (MF), and cellular components (CC).

Screening of diagnostic biomarkers and construction of diagnostic models

The FDEGs were screened using two machine learning algorithms: Support Vector Machine Recursive Feature Elimination (SVM-RFE) and Least Absolute Shrinkage and Selection Operator (LASSO) regression. The former is used for classification and regression analysis, implemented through the 'e1071' package to select and identify genes with high discriminative power[16]. The latter exhibits superiority in evaluating high-dimensional data and utilizes the 'glmnet' package to perform variable selection through regularization[17]. Subsequently, the intersection genes between the two methods were used for logistic regression analysis. Four specific genes (AGPS, BRD4, RBMS1, and EGR1) were identified as diagnostic biomarkers, which showed positive results in both univariate and multivariate examinations. An ROC curve was constructed to preliminarily evaluate the diagnostic biomarkers' effectiveness. A columnar diagram risk prognosis model was constructed using the 'rms' package, and a nomogram was employed to assess the concordance between the observed and predicted values[18]. Lastly, a decision curve analysis (DCA) was conducted to assess the clinical advantages of the model.

GSEA and GSVA of diagnostic biomarkers

The c2.cp.kegg.v7.0.symbols.gmt was downloaded from the MsigDB database as the reference gene set. The 'clusterProfiler' package was utilized to perform gene set enrichment analysis (GSEA) to determine the changes in pathway and biological process activity in the diagnostic biomarker dataset samples[19]. Gene set variation analysis (GSVA) converts the expression matrices of individual genes into expression matrices for specific gene sets[14]. The 'GSVA' package was utilized to further analyze pathway differences among diagnostic biomarkers. A significance threshold of $P < 0.05$ was utilized to identify enriched pathways.

Immune cell infiltration

CIBERSORT is a deconvolution algorithm, widely used for assessing immune cell types in the microenvironment[20]. Using this algorithm, matrix data of immune cell infiltration (22 different cell types) in the synovial tissues of OA and HC were extracted. Subsequently, the 'ggplot2' package was utilized to generate violin plots for visualizing the discrepancies in immune cell infiltration between the two groups[21].

Infiltrating immune cell correlation analysis

Spearman's correlation analysis was conducted to explore the association between the diagnostic biomarkers and immune cell infiltration in the synovial tissue. The outcomes of the analysis were represented graphically utilizing the 'ggplot2' package.

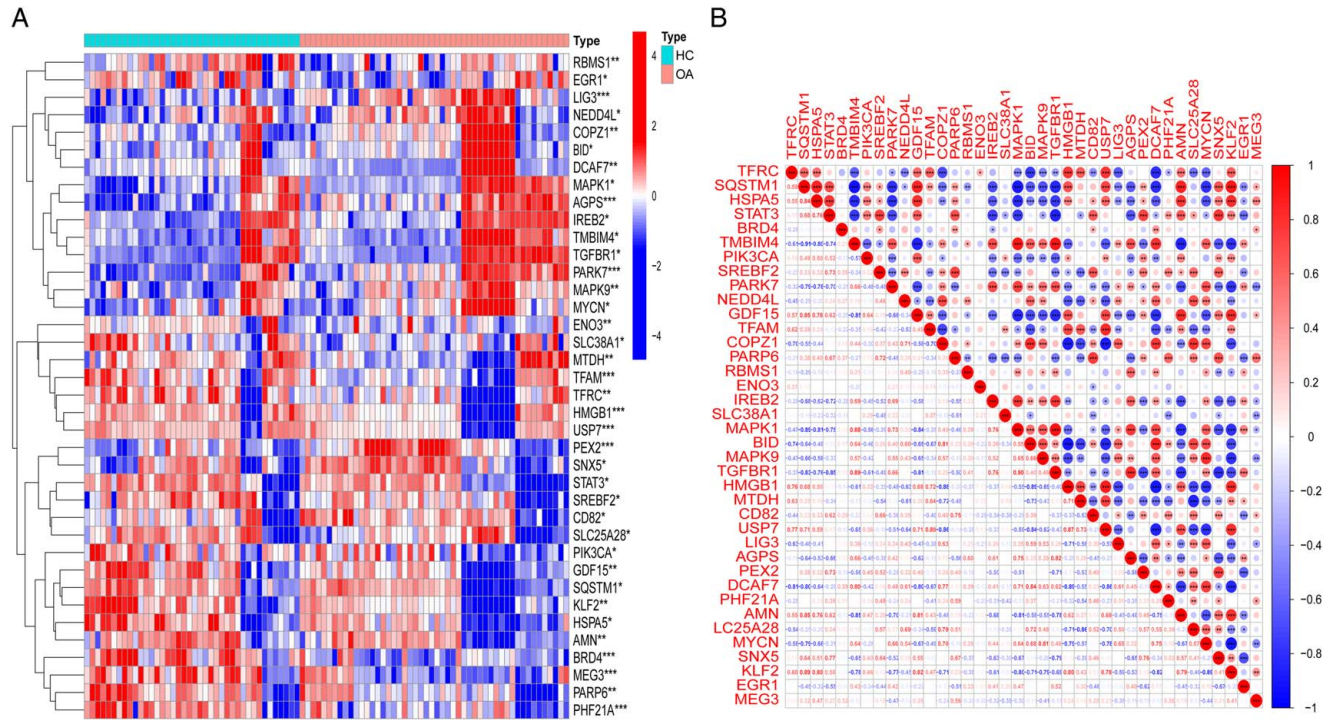

Figure 1. Expression and correlation of FDEGs. (A) The heatmap displays the presentation of FDEGs in OA and HC group synovial tissues. (B) Spearman correlation analysis of FDEGs.

Differential analysis of specific genes

Extract the variance in the presentation of the diagnostic biomarkers in OA and HC synovial tissues using the 'limma' package and visualize the results using the 'ggpubr' package.

Preparation of clinical samples

Synovial samples were collected from three patients with OA treated with arthroplasty and one patient with an amputation due to a car accident injury.

Western blotting analyze

The cells were lysed using RIPA lysis buffer supplemented with protease inhibitors (Beyotime Biotech#P0013B). The proteins were separated by 6 or 10% SDS-PAGE and transferred onto PVDF membranes. Sealing in 5% skimmed milk, the membranes were incubated with primary antibodies against AGPS (1:1000, MA5-28603), BRD 4 (1:1000, PA5-100998), RBMS 1 (1:1000, MA5-27025), ERG 1 (1:1000, MA5-26245), and GAPDH (1:3000, MA1-16757) overnight at 4°C. All antibodies were rabbit polyclonal antibodies from Invitrogen, China. The membranes were then incubated with secondary antibodies at 37°C for 2 h and the protein bands were visualized using a microplate chemiluminescence system (Share-BIO, SB-WB012).

Results

Expression and correlation analysis of FDEGs in OA

Extract the expression matrix of 728 FRG genes from the OA group and the HC group. Visualize the distribution of FDEGs in the OA and HC groups in Figure 1A using a heatmap. Out of the 38 FDEGs that were selected, 16 genes showed significant upregulation, while 22 genes displayed significant downregulation. Figure 1B displays the correlation among the 38 FDEGs.

Functional enrichment analysis of FDEGs

GO enrichment analysis of BP suggests significant enrichment of these genes in processes such as regulation of autophagy, peptidyl – serine phosphorylation, peptidyl – serine modification. In terms of CC, these genes may be involved in important components of organelle membranes. MF suggests that these genes are associated with protein serine/threonine kinase activity, lyase activity, and ubiquitin protein ligase binding (Fig. 2A, B). The KEGG analysis results indicate that these genes are mainly associated with the FoxO signaling pathway, hepatitis B, and pathways related to lipid metabolism and atherosclerosis (Fig. 2C, D).

Screening for diagnostic biological markers

Using the LASSO algorithm and conducting 10-fold cross-validation (Fig. 3A, B), the number of genes corresponding to the minimum cross-validation error was determined to be 16, including: BRD4, PIK3CA, RBMS1, ENO3, IREB2, SLC38A1, MTDH, CD82, LIG3, AGPS, PEX2, DCAF7, AMN, SNX5, EGR1, and MEG3. By employing the SVM-RFE algorithm and conducting 10-fold cross-validation (Fig. 3C, D), the optimal number of genes corresponding to the minimum cross-validation error was selected. In total, 11 FDEGs were identified, namely: AGPS, BRD4, RBMS1, IREB2, EGR1, AMN, CD82, MEG3, DCAF7, ENO3, and SLC38A1. The intersection of the

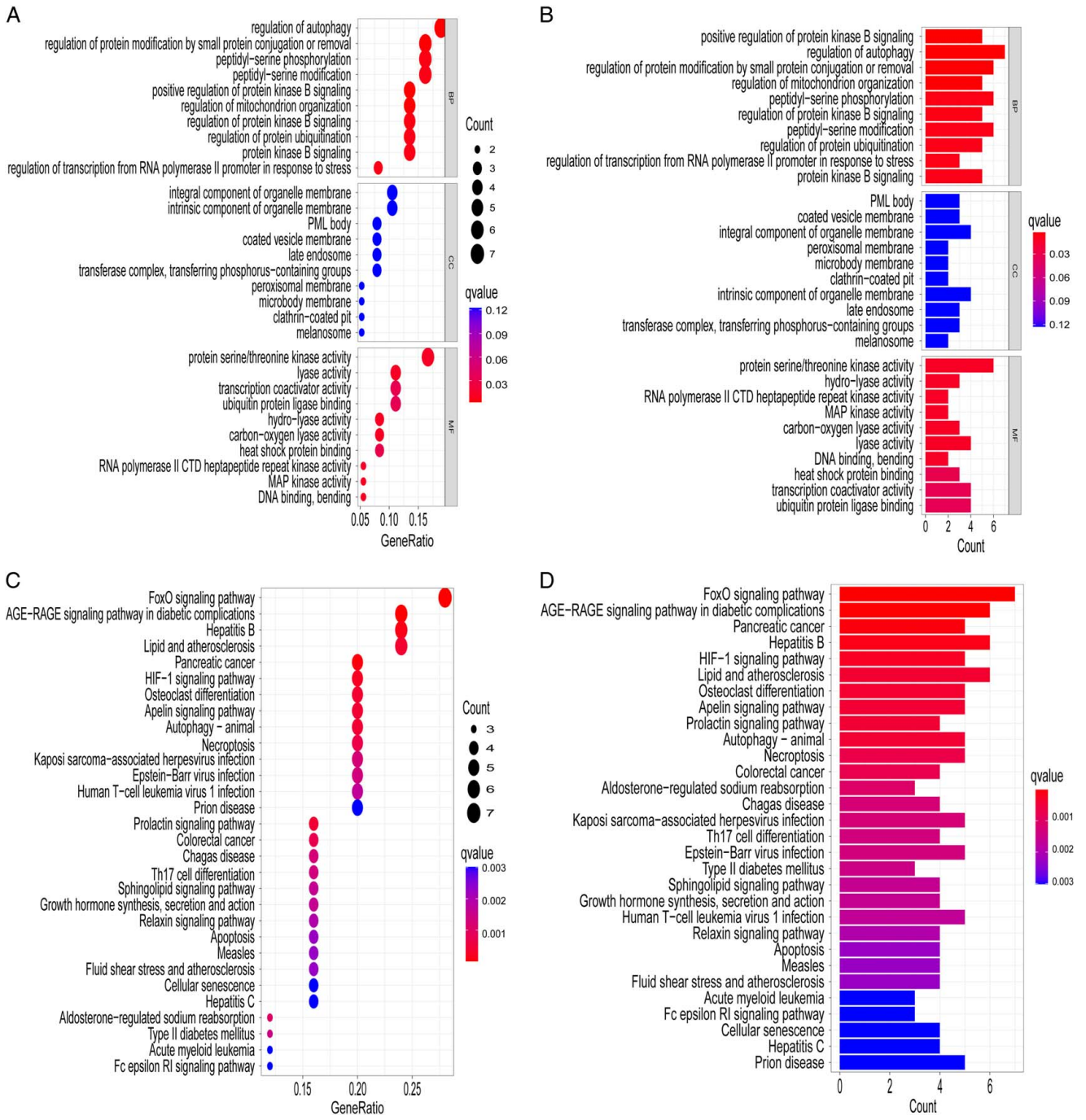

Figure 2. Enrichment results of Gene Ontology (GO) and Kyoto Encyclopedia of Genes and Genomes (KEGG). (A, B) GO bubble chart and bar graph. (C, D) KEGG bubble chart and KEGG bar graph.

two algorithms yielded 11 FDEGs (Fig. 3E). Utilizing logistic regression analysis, four specific genes were identified as positive in both univariate and multivariate analyses, namely: AGPS, BRD4, RBMS1, and EGR1. These genes were then selected as diagnostic biomarkers (Table 1).

Predictive model building and evaluation

The ROC curve and corresponding AUC values were utilized to assess the specificity and sensitivity of AGPS, BRD4, RBMS1, and EGR1 in diagnosing OA. The AUC value was 0.962 (Fig. 4A). A nomogram that was constructed based on these four specific genes to predict the probability of OA (Fig. 4B). Each feature gene in the nomogram corresponds to a score, and by adding up the scores of all feature genes, a whole score is obtained, which compares to different risk levels of OA. The calibration curve confirms the predictive accuracy of the nomogram in estimating the progression of OA (Fig. 4C). The DCA plot, the use of the nomogram can benefit OA patients in clinical settings (Fig. 4D).

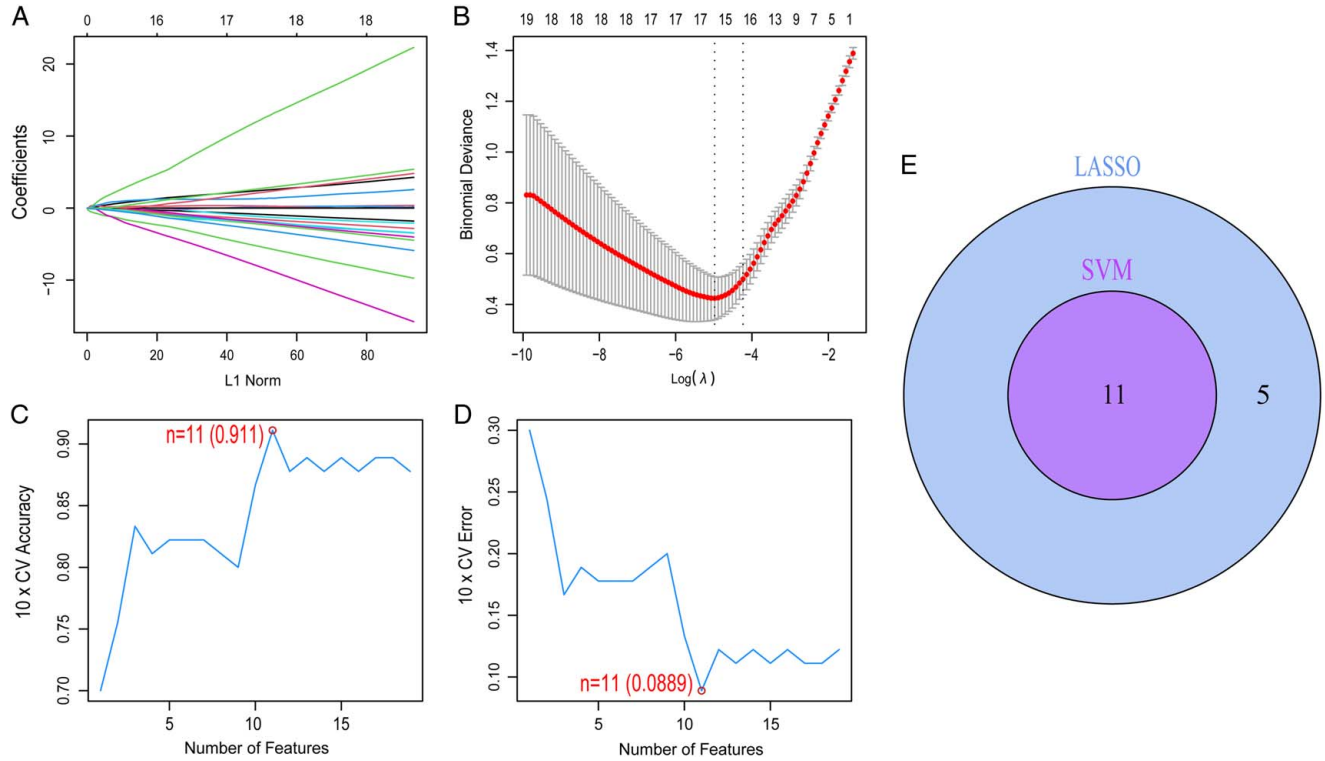

Figure 3. Utilization of Lasso regression and SVM methods to screen diagnostic biomarker genes. (A, B) demonstrate the Lasso regression model and corresponding cross-validation plots. (C, D) display the accuracy and cross-validation error plots for the SVM algorithm. (E) illustrates a Venn diagram displaying the reliable biomarkers identified through LASSO and SVM-RFE.

GSEA and GSVA analysis in order to reveal the potential function of specific genes

GSEA and GSVA are performed based on each specific gene. The analysis shows that when AGPS expression is high, there is an activation of the TGF-β signaling pathway and MAPK signaling pathway, whereas when AGPS expression is low, there is an activation of Parkinson's disease and oxidative phosphorylation pathways (Fig. 5A). In the case of high BRD4 expression, interactions between neuroactive ligands and receptors are active, while in the case of low expression, Parkinson's disease and oxidative phosphorylation are active (Fig. 5C).The TGF-β signaling pathway is active in the case of high RBMS1 expression, and Parkinson's disease and oxidative phosphorylation are active in the case of low expression (Fig. 5E). Cytokine-cytokine receptor interactions were active in the case of high EGR1 expression, and arginine and proline metabolism and Parkinson's disease were active in the case of low expression (Fig. 5G). The GSVA results indicate that β-alanine metabolism and RNA polymerase function are active under high AGPS expression, and the renin-angiotensin system and the biosynthesis of valine, leucine, and isoleucine are active under low expression (Fig. 5B). Propionate metabolism and starch and sucrose metabolism were active under high expression of BRD4, and steroid hormone biosynthesis was active under low expression

Table 1

Logistic analysis results of LASSO and SVM-REF intersection genes

		Univariate analysis		Multivariate analysis	
Characteristics	**Total (*N*)**	**Odds ratio (95% CI)**	***P***	**Odds ratio (95% CI)**	***P***
AGPS	90	5.670 (4.741–6.599)	< 0.001	248.214 (244.751–251.676)	0.002
BRD4	90	0.130 (– 0.802–1.063)	< 0.001	0.051 (– 2.184–2.286)	0.009
RBMS1	90	0.315 (– 0.673–1.304)	0.022	0.004 (– 3.654–3.663)	0.003
IREB2	90	1.222 (0.956–1.487)	0.140		
EGR1	90	0.631 (0.217–1.045)	0.029	5.381 (4.072–6.689)	0.012
AMN	90	0.683 (0.343–1.023)	0.028	2.490 (1.554–3.426)	0.056
CD82	90	1.433 (1.068–1.798)	0.053	9.622 (8.339–10.905)	< 0.001
MEG3	90	0.319 (– 0.230–0.868)	< 0.001	0.149 (– 1.856–2.154)	0.063
DCAF7	90	0.910 (0.423–1.397)	0.705		
ENO3	90	0.833 (0.606–1.060)	0.114		
SLC38A1	90	0.398 (– 0.351–1.147)	0.016	0.157 (– 2.131–2.445)	0.112

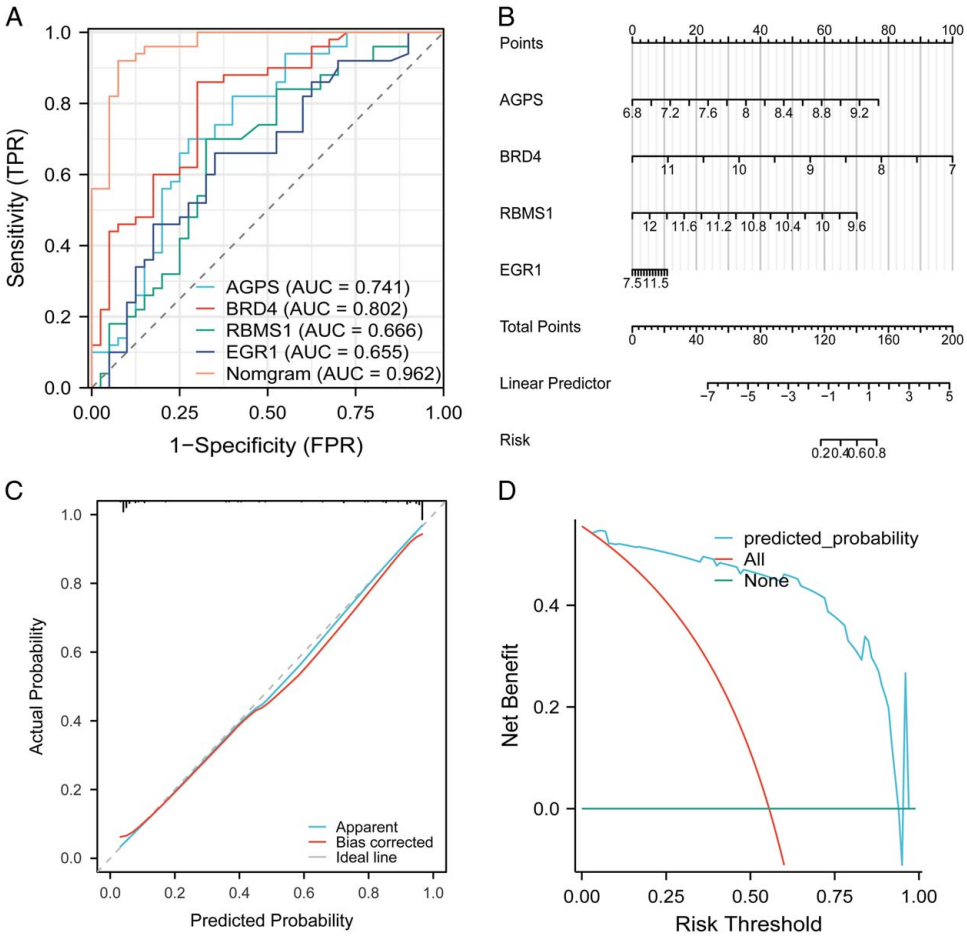

Figure 4. Assessment of diagnostic biomarkers. (A) The ROC curve and its corresponding AUC value are shown. (B) A nomogram risk prediction model is presented. (C) The calibration curve is illustrated. (D) The DCA curve is displayed.

(Fig. 5D). Drug metabolism-cytochrome P450 and cytochrome metabolism of xenobiotics was active in the case of high RBSM1 expression, and limonene and pinene degradation and sphingolipid metabolism was active in the case of low expression (Fig. 5F). RNA polymerase and porphyrins and chlorophylls of metabolism was active in the case of high EGR1 expression, and metabolism of linoleic acid and cytokine-cytokine receptor interactions was active in the case of low expression (Fig. 5H). In summary, the results of both GSEA and GSVA confirm that these diagnostic biomarker genes contribute to the process of metabolic proliferation.

Correlation between specific genes and co-expression of OA immune cell infiltration

The CIBERSORT algorithm was utilized to calculate the proportions of immune cell infiltration in the synovial tissues of both the OA and HC groups (Fig. 6A). In comparison to the HC group, the OA group demonstrated a more heightened infiltration of gamma delta T cells ($P = 0.026$), while the HC group had a more heightened infiltration of follicular helper T cells ($P = 0.001$) and eosinophils ($P = 0.015$) in their synovial tissues. The correlation among four particular genes and 22 infiltrating immune cells existed computed (refer to Fig. 6B). The outcomes demonstrated that AGPs were positively likened with resting dendritic cells and eosinophils and negatively likened with CD8 + T cells and gamma delta T cells. BRD4 was positively likened with resting dendritic cells, M2 macrophages, and monocytes and negatively likened with M0 macrophages, resting mast cells, and gamma delta T cells. RBMS1 was positively likened with eosinophils and M1 macrophages. EGR1 was positively likened with CD4 + memory resting T cells, CD4 + naïve T cells, and negatively likened with neutrophils.

Differential analysis of specific genes

Differential analysis of the expression of AGPS, BRD4, RBMS1, and EGR1 in the synovial membrane of the OA and HC groups (Fig. 7A–D). Significantly higher expression of AGPS in OA synovium ($P = 9.5e\text{-}05$), significantly lower expression of BRD4 in OA synovium ($P = 9.7e\text{-}07$), significantly lower expression of RBMS1 in OA synovium ($P = 0.0071$) and significantly lower expression of EGR1 in OA synovium ($P = 0.012$) could be seen—further evidence of the value of specific genes for the diagnosis and treatment of OA.

Western blotting analyze

Western blot analyses revealed a significant upregulation of AGPS in the synovial tissues of OA patients in comparison to those of healthy individuals. Concurrently, the expression levels

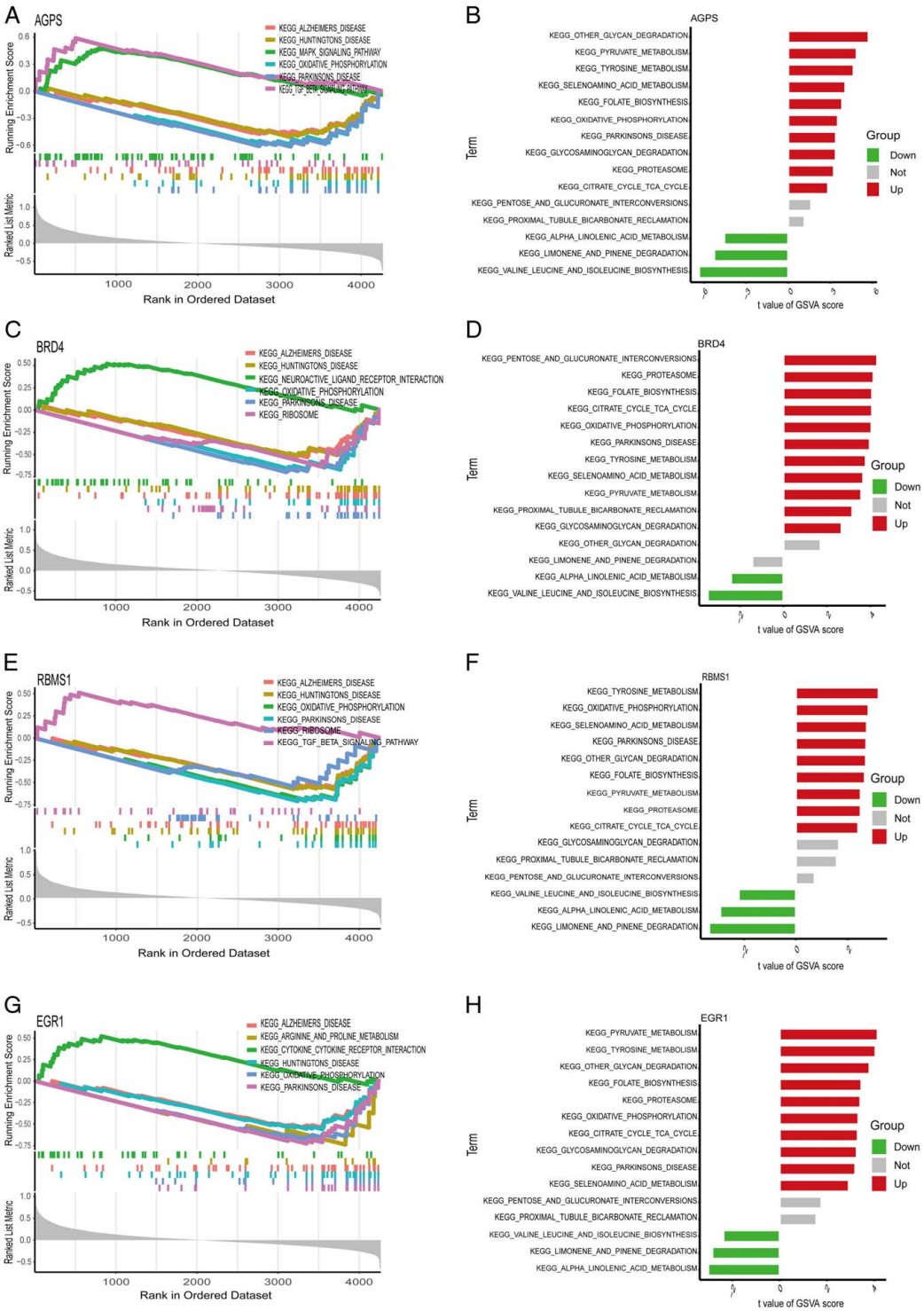

Figure 5. Diagnostic biomarker genes for GSEA and GSVA. (A, B) AGPS; (C, D) BRD4; (E, F) RBMS1; (G, H) EGR1.

of BRD4, RBMS1, and EGR1 were notably downregulated, aligning with our earlier data analysis (Fig. 8).

Discussion

OA is a disease that affects the entire joint. It does not simply affect a single tissue, but rather involves a pathological process affecting the entire joint[22]. In the past, most research has focused solely on disparities in the articular cartilage of the joint, while overlooking the important role of soft tissue surrounding the knee joint[23]. Nowadays, there is relevant research indicating that changes in the synovium are present throughout the course of OA[24]. In particular, persistent low-grade inflammation of the synovium in early stages of OA may be the starting point for

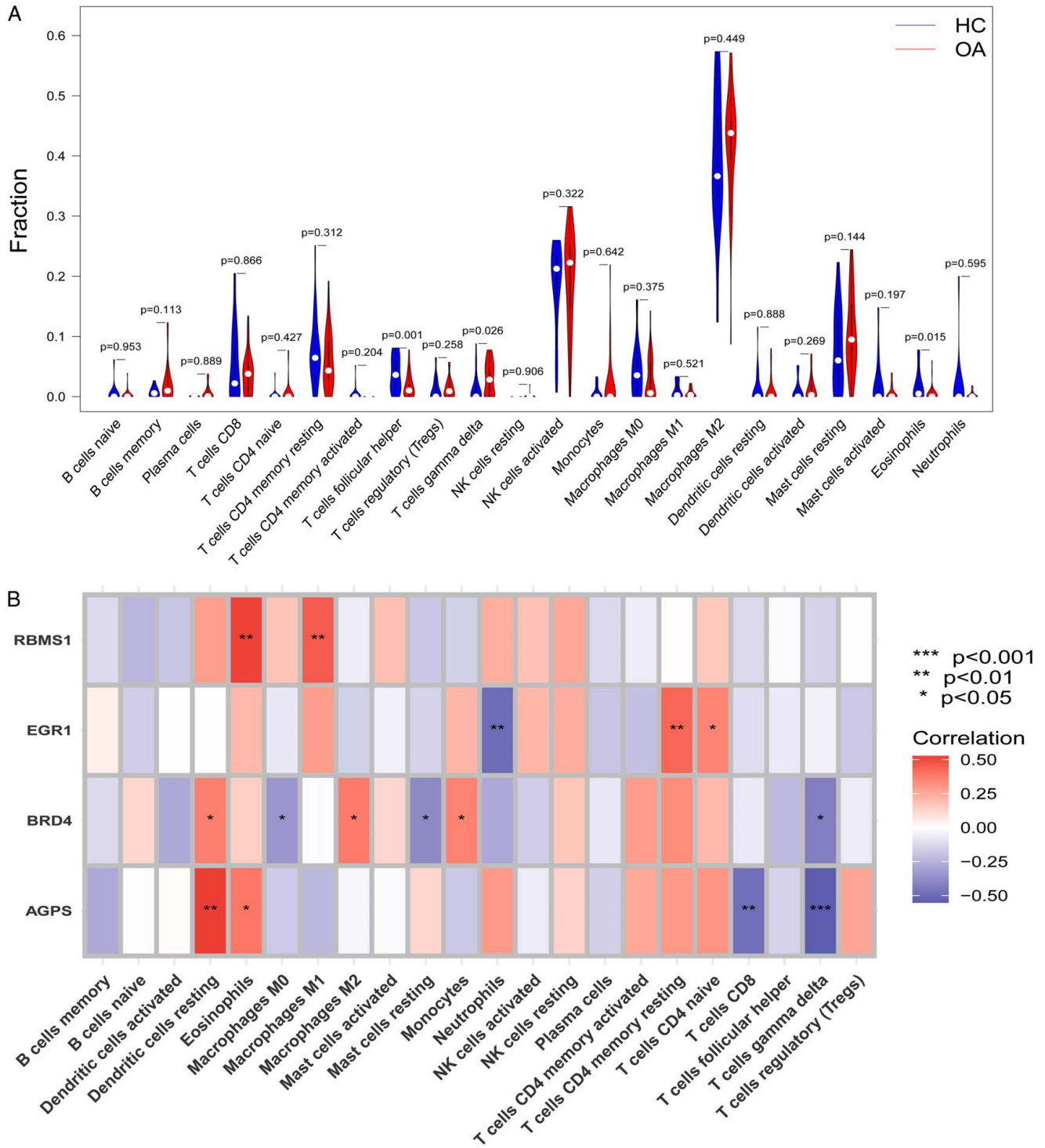

Figure 6. Evaluation and Visualization of Infiltration by Immune Cells. (A) Violin Plot Depicting the Proportions of 22 Types of Immune Cells. (B) Relationship between four specific genes and immune cell infiltration.

inducing irreversible joint damage and changes[25]. Therefore, studying synovitis and its related pathogenic mechanisms is especially important. Recently, ferroptosis has been extensively studied and has made significant progress in various disease areas such as cardiovascular disease, kidney failure, leukemia, and others[26–28]. However, its role and impact on synovitis in OA remain unclear.

This study obtained 90 synovial tissue samples (OA and HC) and 728 latest FRG data from GEO and FerrDB databases, and obtained 38 FDEGs through bioinformatics analysis. To observe

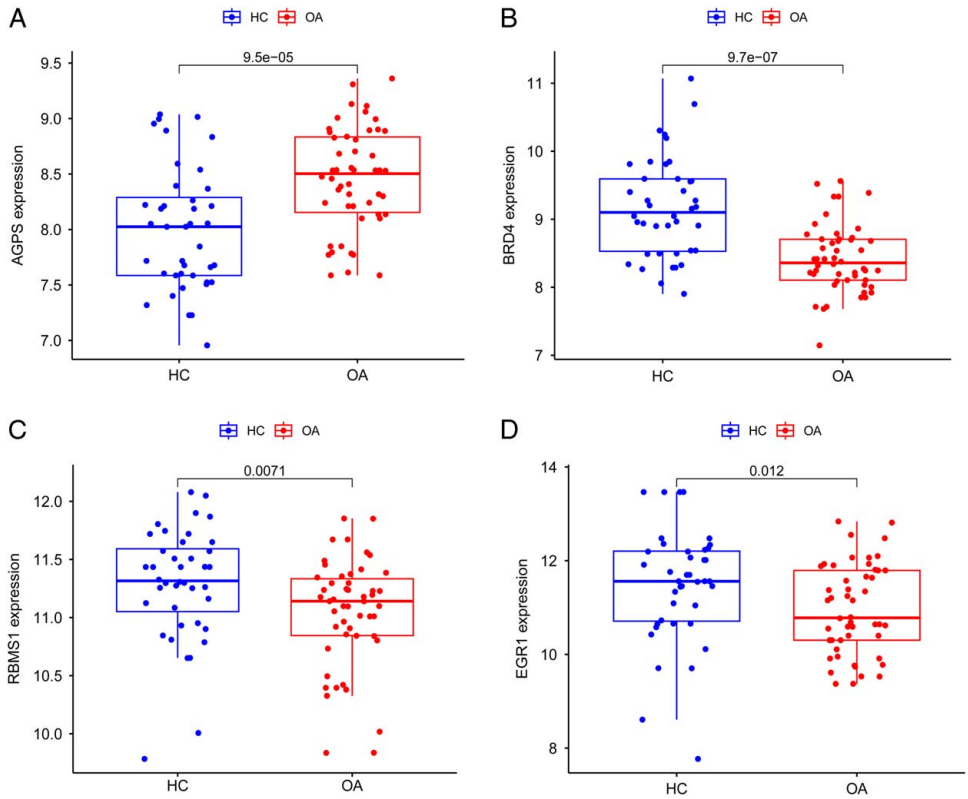

Figure 7. Box diagram of differential expression of single specific gene (A) AGPS (B) BRD4 (C) RBMS1 (D) ERG1.

the function and pathways of FDEGs, we performed GO and KEGG enrichment analyses. Regarding BP, GO analysis indicated that FDEGs have mostly been enriched in autophagy regulation. In terms of CC, they may be involved in important components of organelle membranes. MF was mainly connected to protein serine/threonine kinase activity. The KEGG results suggest that FDEGs are primarily enriched in the FoxO signaling pathway. The primary outcomes of both enrichment analyses revealed the consistency of FDEGs in regulating cellular autophagy. Studies have shown that FoxO is concerned with regulating cellular ageing mechanisms such as antioxidant stress and autophagy regulation. Cellular ageing is closely related to inflammation and cartilage deterioration in OA[29]. Therefore, the outcomes of the two enrichment analyses of FDEGs contribute to a better knowledge of the pathogenesis underlying OA. Correspondingly, we demonstrated the correlations between FDEGs, which will facilitate further studies targeting FDEGs. Compared to previous studies, we used for the first time LASSO and SVM-RFE machine learning algorithms to filter the FDEGs, which greatly improved the representativeness of the selected genes[30]. Later , using logistic regression analysis, univariate and multivariate conducted on the intersection genes between the two algorithms were performed. This further enhances the practical clinical application value of the screened genes. The four specific genes, including AGPS, BRD4, RBMS1, and EGR1, which were positive in both univariate and multivariate analyses, were finally selected as diagnostic biomarkers. The ROC curve and nomogram clinical risk prognostic model show that the four diagnostic biomarker genes have a good diagnostic and therapeutic effect on OA.

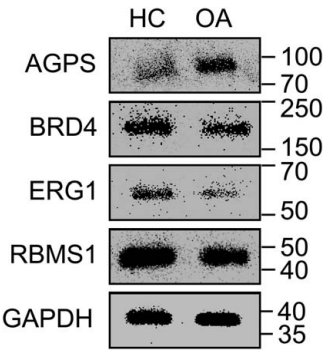

Figure 8. Western blot analysis results for AGPS, BRD4, RBMS1, and EGR1.

To find out the potential functions of the diagnostic biomarkers, we performed GSEA and GSVA analysis and found that their functions mainly focus on cell growth, differentiation, and apoptosis. Among them, the most typical pathways are the TGF-β signaling pathway and the MAPK signaling pathway. Earlier research has demonstrated that as synovial inflammation progresses, the expression levels of factors that induce synovial fibrosis may be upregulated, and the main reason for this is the activation of the TGFβ pathway[25,31]. The MAPK signaling pathway can affect the progression of OA by enabling the phenotypic transformation of synovial macrophages[32]. This provides guidance for revealing the potential mechanisms between

the four diagnostic biomarker genes and OA. In addition, some studies have linked ferroptosis to rheumatoid immune illnesses[33]. Therefore, using the CIBERSORT algorithm, matrix data of immune cell infiltration (22 different cell types) of OA and HC synovial samples were extracted. We built a relationship between particular genes and the co-expression of immune cell infiltration in OA using Spearman correlation analysis. Compared to the HC group, the OA group demonstrated a more heightened infiltration of gamma delta T cells ($P = 0.026$). In contrast, the HC group had a more heightened infiltration of eosinophils ($P = 0.015$). The outcomes demonstrated that AGPs were positively likened with eosinophils ($P < 0.05$) and negatively likened with gamma delta T cells ($P < 0.001$). BRD4 was negatively likened to gamma delta T cells ($P < 0.05$). RBMS1 was positively likened to eosinophils ($P < 0.01$). EGR1 was positively likened with CD4 + memory resting T cells ($P < 0.01$) and negatively likened with neutrophils ($P < 0.01$). This demonstrates an association between four specific genes and OA immune cell infiltration. However, the exact mechanisms of their interaction still need to be further investigated. Finally, we have successfully validated the differential expression of four diagnostic biomarker genes in synovial tissue samples from OA and HC. Significantly higher expression of AGPS in OA synovium ($P = 9.5e-05$), while the expression of BRD4 ($P = 9.7e-07$), RBMS1 ($P = 0.0071$), and EGR1 ($P = 0.012$) was significantly decreased in the synovial tissue of OA. Western blot analyses revealed a significant upregulation of AGPS in the synovial tissues of OA patients in comparison to those of healthy individuals. Concurrently, the expression levels of BRD4, RBMS1, and EGR1 were notably downregulated. This further confirms their diagnostic and therapeutic value for OA. This further confirms their diagnostic and therapeutic value for OA.

However, there are several limitations to this study. For starters, the amount of the sample may lead to certain biases. Secondly, further in vivo and in vitro experiments are needed to validate these biomarker genes' diagnostic and therapeutic value.

Conclusion

This work identified four FDEGs as potential diagnostic biomarker genes for OA synovitis, including two ferroptosis-driving genes (AGPS and EGR1) and two ferroptosis- suppressor genes (BRD4 and RBMS1). Moreover, the construction of a diagnostic biomarker risk prognostic model can facilitate early diagnosis of OA, evaluation of functional recovery, and guidance for subsequent treatment.

Ethical approval

The protocol for sample collection received approval from the Ethics Committee of the Second Affiliated Hospital of Anhui Medical University and adhered to pertinent guidelines and regulations. No. YX2022-104.

Consent

Not applicable.
Our study does not involve privacy related to patients' names, images, etc. All authors declare that informed consent of patients was not required for this experimental study.

Sources of funding

Not applicable.

Author contribution

Y.Y.: completed the experiments and manuscript writing; J.H.: completed the data collection; and W.C.: provided experimental guidance.

Conflicts of interest disclosure

The authors declare that they have no competing interests.

Research registration unique identifying number (UIN)

Not applicable.

Guarantor

Yiqun Yan.

Data availability statement

The datasets generated and/or analyzed during the current study are available in the GEO database (https://www.ncbi.nlm.nih.gov/geo).

Provenance and peer review

Not applicable.

References

[1] Hunter DJ, Bierma-Zeinstra S. Osteoarthritis. Lancet 2019;393:1745–59.
[2] Fang T, Zhou X, Jin M, *et al*. Molecular mechanisms of mechanical load-induced osteoarthritis. Int Orthop 2021;45:1125–36.
[3] Usher KM, Zhu S, Mavropalias G, *et al*. Pathological mechanisms and therapeutic outlooks for arthrofibrosis. Bone Res 2019;7:9.
[4] Charlier E, Deroyer C, Ciregia F, *et al*. Chondrocyte dedifferentiation and osteoarthritis (OA). Biochem Pharmacol 2019;165:49–65.
[5] Fujii Y, Liu L, Yagasaki L, *et al*. Cartilage Homeostasis and Osteoarthritis. Int J Mol Sci 2022;23.
[6] Dixon SJ, Lemberg KM, Lamprecht MR, *et al*. Ferroptosis: an iron-dependent form of nonapoptotic cell death. Cell 2012;149:1060–72.
[7] Stockwell BR. Ferroptosis turns 10: Emerging mechanisms, physiological functions, and therapeutic applications. Cell 2022;185:2401–21.
[8] Li N, Yi X, He Y, *et al*. Targeting Ferroptosis as a Novel Approach to Alleviate Aortic Dissection. Int J Biol Sci 2022;18:4118–34.
[9] Wang Y, Zhang M, Bi R, *et al*. ACSL4 deficiency confers protection against ferroptosis-mediated acute kidney injury [J]. Redox Biol 2022;51 102262.
[10] Lin Z, Song J, Gao Y, *et al*. Hypoxia-induced HIF-1alpha/lncRNA-PMAN inhibits ferroptosis by promoting the cytoplasmic translocation of ELAVL1 in peritoneal dissemination from gastric cancer. Redox Biol 2022;52:102312.
[11] Miao Y, Chen Y, Xue F, *et al*. Contribution of ferroptosis and GPX4's dual functions to osteoarthritis progression. EBioMedicine 2022;76: 103847.
[12] Alborzinia H, Florez AF, Kreth S, *et al*. MYCN mediates cysteine addiction and sensitizes neuroblastoma to ferroptosis. Nat Cancer 2022; 3:471–85.
[13] Leek JT, Johnson WE, Parker HS, *et al*. The Sva package for removing batch effects and other unwanted variation in high-throughput experiments[J].Bioinformatics2012;28:882–3.

[14] Ritchie ME, Phipson B, Wu D, *et al*. Limma powers differential expression analyses for RNA-sequencing and microarray studies. Nucleic Acids Res 2015;43:e47.
[15] Wu T, Hu E, Xu S, *et al*. clusterProfiler 4.0: A universal enrichment tool for interpreting omics data. Innovation (Camb) 2021;2:100141.
[16] Huang S, Cai N, Pacheco PP, *et al*. Applications of support vector machine (SVM) learning in cancer genomics. Cancer Genomics Proteomics 2018;15:41–51.
[17] Zhao E, Xie H, Zhang Y. Predicting diagnostic gene biomarkers associated with immune infiltration in patients with acute myocardial infarction. Front Cardiovasc Med 2020;7:586871.
[18] Yu Y, Wang L, Li Z, *et al*. Long noncoding RNA CRNDE functions as a diagnostic and prognostic biomarker in osteosarcoma, as well as promotes it progression via inhibition of miR-335-3p. J Biochem Mol Toxicol 2021;35:e22734.
[19] Langfelder P, Horvath S. WGCNA: an R package for weighted correlation network analysis. BMC Bioinform 2008;9:559.
[20] Newman AM, Liu CL, Green MR, *et al*. Robust enumeration of cell subsets from tissue expression profiles. Nat Methods 2015;12:453–7.
[21] Liu W, Xie X, Qi Y, *et al*. Exploration of immune-related gene expression in osteosarcoma and association with outcomes. JAMA Network Open 2021;4:e2119132.
[22] Wei Q, Kong N, Liu X, *et al*. Pirfenidone attenuates synovial fibrosis and postpones the progression of osteoarthritis by anti-fibrotic and anti-inflammatory properties in vivo and in vitro. J Transl Med 2021;19:157.
[23] Sanchez-Lopez E, Coras R, Torres A, *et al*. Synovial inflammation in osteoarthritis progression. Nat Rev Rheumatol 2022;18:258–75.
[24] Mathiessen A, Conaghan PG. Synovitis in osteoarthritis: current understanding with therapeutic implications. Arthritis Res Ther 2017;19:18.
[25] Remst DF, Blaney Davidson EN, Van Der Kraan PM. Unravelling osteoarthritis-related synovial fibrosis: a step closer to solving joint stiffness. Rheumatology (Oxford) 2015;54:1954–63.
[26] Liu Y, Wang J. Ferroptosis, a rising force against renal fibrosis. Oxid Med Cell Longev 2022;2022:7686956.
[27] Li Z, Zhang C, Liu Y, *et al*. Diagnostic and predictive values of ferroptosis-related genes in child sepsis. Front Immunol 2022;13:881914.
[28] Fan X, Li A, Yan Z, *et al*. From iron metabolism to ferroptosis: pathologic changes in coronary heart disease. Oxid Med Cell Longev 2022;2022:6291889.
[29] Akasaki Y, Hasegawa A, Saito M, *et al*. Dysregulated FOXO transcription factors in articular cartilage in aging and osteoarthritis. Osteoarthritis Cartilage 2014;22:162–70.
[30] Xia L, Gong N. Identification and verification of ferroptosis-related genes in the synovial tissue of osteoarthritis using bioinformatics analysis. Front Mol Biosci 2022;9:992044.
[31] Van Der Kraan PM. The changing role of TGFbeta in healthy, ageing and osteoarthritic joints. Nat Rev Rheumatol 2017;13:155–63.
[32] Zhou F, Mei J, Han X, *et al*. Kinsenoside attenuates osteoarthritis by repolarizing macrophages through inactivating NF-kappaB/MAPK signaling and protecting chondrocytes. Acta Pharm Sin B 2019;9:973–85.
[33] Zhao T, Yang Q, Xi Y, *et al*. Ferroptosis in rheumatoid arthritis: a potential therapeutic strategy. Front Immunol 2022;13:779585.